Trends in Biomaterials and Artificial Organs
www.biomaterials.org.in/tibao
ISSN 0971-1198
https://doi.org/10.5281/zenodo.16959268

Original Article

Electrophoretic Deposition of Titania Based Coating on Ti-6Al-4V Implants for Orthopaedic Applications

K.K. Anavadya, S. Ajay Niranjan, U. Vijayalakshmi*

Department of Chemistry, School of Advanced Sciences, Vellore Institute of Technology, Vellore 632014, India

Received: *3 March 2025*
Accepted: *22 April 2025*
Published online: *26 August 2025*

Keywords: *graphene oxide, titanium dioxide, coatings, electrophoretic deposition, orthopaedic implants*

Titanium dioxide (TiO_2) is a propitious biomaterial for orthopaedic implants ascribed to its, biocompatibility, inertness and non-toxic nature. Graphene oxide (GO) incorporated rutile titanium dioxide has the combined properties of both, with enhanced performance and functionality in biomedical field. It comports as an ideal coating for orthopaedic implant by improving the mechanical strength, thermal stability and antimicrobial properties. GO is synthesized by modified Hummer's method. The GO incorporated with TiO_2 is fabricated by sol-gel method. The preliminary studies of synthesized composite powder were examined with XRD, FTIR, UV-Vis spectroscopy, photoluminescence, scanning electron microscopy, and Raman spectroscopy. The synthesized GO doped TiO_2 at optimized weight percentage was coated on titanium alloy implant using electrophoretic deposition technique. Optimized coating is selected by varying voltage parameters with fixed time duration. Uniform and crack free coatings are observed at 80V at 180 seconds.

Introduction

Materials contrived to interact with biological systems and have the ability to induce a physiological response are termed as biomaterials. All biomaterials should possess high volume-surface area, porosity, host specificity, surface modifiable and bioactivity. Over time biomaterials have undergone tremendous evolution from first generation biomaterials which are materials that are only biocompatible, mostly inert to fourth generation biomaterials which are biomimetic materials such as tissue engineered scaffolds [1]. Implants are second generation biomaterials which are biocompatible, bioresorbable and bioactive. Implants in medical field is the term used for devices manufactured for the replacement of a biological part in a person. If the implant is supplanted by prosthesis for bone tissues, cartilage, joint, it is then identified as "orthopaedic implant" [2-4]. Prosthetic implant is a device which restores the function of the joint or cartilage by providing mechanical support or complete replacement of the skeletal tissue deformed by unprecedented situations specifically accidents or sometimes even diseases like osteoarthritis. The prosthetics are usually made of metals, ceramics, polymers and composites. The metals (d-block elements) such as iron, zinc, copper, lead, silver, etc was used in the manufacturing process of implants despite their adverse effect due to lack of technology advancement but now in recent times with rapid development of science and technology biocompatible materials like cobalt chromium alloys, stainless steel and doped nanocomposites are being used in production of prosthetics.

Nanocomposites those are doped with graphene have plenteous advantages over other nanocomposites due to reformed mechanical strength, electrical conductivity, flexibility, thermal stability, stimuli response and membrane separation characteristics [5]. The oxidised two-dimensional (2D) sheet of carbon atoms (sp^2 hybridised) in the form of honeycomb structure is the configuration of graphene. The graphene synthesis is strenuous as a consequence of the poor solubility leading to formation of agglomeration in solution caused by Van der Waals interaction. To get over this constraint, mostly graphene oxide (GO) or reduced graphene oxide (rGO) is utilized alternate to graphene. The oxidized form of graphene, with single monomolecular layer of graphite with various oxygen containing functionalities such as epoxide, carbonyl, carboxyl and hydroxyl groups constructs graphene oxide. Reduction of GO by suitable process yield reduced graphene oxide (rGO) which almost resembles graphene but

* *Coresponding author*
E-mail address: vijayalakshmi.u@vit.ac.in (*Dr. Vijayalakshmi U. Department of Chemistry, School of Advanced Sciences, Vellore Institute of Technology, Katpadi, Vellore 632014, Tamil Nadu, India)*

contains structural defects, heteroatoms and residual oxygen. Graphene oxide is one of the best suited compounds to enhance the hydrophilicity, mechanical strength, thermal stability, improved fouling resistance, high permeability of a membrane when incorporated [6,7]. These properties are attributed by sp^3 carbons surrounding the sp^2 carbons and oxygen containing hydrophilic groups. GO finds plentiful applications in nanocomposite materials, polymer composite materials, biomedical applications, catalysis, biosensors, drug delivery etc. Amidst the numerous approaches of graphene oxide synthesis namely Hummer's method, Tour's method, Brodie's method, and Staudenmaier's method, we prefer the most prevailing method which is modified Hummer's method that exhibits cost effectiveness and reasonably shorter processing time with graphite as precursor.

Titanium dioxide (TiO_2) exists in three prominent phases namely rutile, anatase and brookite. Due to the variations in spatial configurations, three phases have distinctive features, which because of its higher stability, is primarily chosen in the rutile and anatase phases, which contribute significantly to the thermodynamic stability of the TiO_2. It is an emerging nanomaterial that has conceivable applications in photocatalysis, biomedical field and semiconductors. TiO_2 particles have been garnering substantial interest in wide range of domains due to its exceptional chemical, physical, optical, thermal, mechanical, biocompatible properties, particularly lesser toxicity [1,8,9]. Considering the high biocompatibility, antibacterial, antimicrobial and osteoinductive properties, titanium is an exquisite material for orthopaedic applications. The thin native oxide layer of titanium dioxide film formation abets the metal by amplifying the corrosion, wear and fatigue resistance contributing to biocompatibility.

Doping with materials like graphene oxide, carbon nanotubes (CNT) or lanthanides (cerium, samarium, gadolinium) [4,10,11], TiO_2 offers superiority in mechanical, antimicrobial, and bioactive properties. Of particular significance, GO qualifies as the dopant material attributable to its less toxicity compared to CNTs, thermal stability, larger surface area, charge mobility, photo-stability, and alteration in the band gap with increased surface area by recombination of electron-hole pairs which eventually enhances the photocatalytic disintegration activity of TiO_2. Opting graphene oxide as a dopant to TiO_2 was to improve the mechanical attributes of the implant like hardness, avoid the biofilm formation and further risks by providing maximum anti-bacterial efficiency, better hydrophilicity which aids in better cell adhesion to the implant and enhanced corrosion resistance are some among the major advantages. A multitude of methods like hydrothermal, co-precipitation, solid state reaction, sol-gel synthesis, etc. can be employed in TiO_2 fabrication. In this work, we favour sol-gel process on account of its high precision and control over doping concentration with doping material along with increased phase purity. The GO doped TiO_2 is coated on titanium alloy (Ti-6Al-4V) implant by electrophoretic deposition (EPD). In electrophoretic deposition method by electric field charged particles contained in a colloidal suspension are moved and deposited on the opposite charged substrate producing the intended coated implant [12-14].

Materials and Method

Titanium (IV) isopropoxide ($Ti[OCH(CH_3)_2]_4$) which was the precursor for TiO_2 was procured from Sisco Research Laboratories Private Limited. Glacial acetic acid was obtained from Avra Synthesis Private Limited. Graphite flakes, sodium nitrate, potassium permanganate and hydrogen peroxide were obtained from SD Fine Chemical Limited. The solvent for electrophoretic deposition was isopropyl alcohol procured from HIMEDIA. Polyvinyl pyrrolidine (K-30) and iodine crystals are obtained from Sisco Research Laboratories Pvt. Ltd. The substrate for the electrophoretic deposition was Ti-6Al-4V alloy (Grade 5) of which was cut into 10mm x 10mm x 10mm which is further polished using BAINPOL-ET using SiC grid sheets of 220, 400, 600, 800 and 1000 and mirror polished at the final stage using diamond polishing with grain size 3-4 μm. Electrophoretic deposition was carried out by varying voltage using Aplab regulated DC power L1285 model.

Preparation of graphene oxide

Modified Hummer's method was preferred for graphene oxide synthesis from graphite flakes [6,15-18]. 1g of graphite, 0.5g of $NaNO_3$, 23ml of H_2SO_4 are stirred in ice bath for 30 minutes. Extreme gradual addition of oxidising agent $KMnO_4$ for functionalization was in the ratio of 1:3 with respect to graphite and stirred in ice bath for 1 hour. Subsequently, the solution is stirred at 35°C for 2 hrs followed by addition of 46ml of distilled water slowly to the solution heated for 1 hour at 98°C. Allow the solution to cool and then add 146 ml of distilled water and 10 ml of 30% H_2O_2 to remove excess manganese ions. Finally, washing is carried out with HCl and water and also centrifuged at the 4000rpm repeatedly. The obtained filtrate was dried in oven for 12 hrs, to acquire graphene oxide flakes which was further characterized for purity and other properties.

Synthesis of graphene oxide doped TiO_2

TiO_2 particles was synthesized using sol-gel synthesis [19,20]. Titanium (IV) isopropoxide, glacial acetic acid as the solvent and double distilled water was mixed in the ratio of 1:30:300. Further refluxed for 12 hours at 70°C. Prepared graphene oxide was added to the sol in different weight percentage as 1wt%, 2wt% and 3wt%. The resultant sol was evaporated, slowly forming a precipitate gel which was further dried in oven at 100°C for two hours, then calcined for two hours at 900°C. The synthesized GO-TiO_2 is analysed for other characterizations. The optimized weight percentage of GO doped TiO_2 is further opted for the EPD Coating.

Fabrication process of EPD coatings

The mirror polished Ti-6Al-4V metal alloy substrates were degreased in acetone prior to the EPD coating process [12,13,21,22]. The optimized weight percentage after initial characterizations and haemolytic studies, 3g/L of GO doped TiO_2 was selected and dispersed in 75ml of Isopropyl Alcohol and kept for overnight stirring. PVP acts as a polymeric binder and I_2 was added to the suspension as surfactant. Stainless Steel was used as Anode and degreased Ti-6Al-4V substrate as the cathode at a distance of 10mm apart. A variation in voltage parameters were made with fixed time interval of 180 seconds. The coating was tried for 50V, 60V, 70V and 80V at 180 seconds. The coatings are further sintered at 200°C for 30 minutes. The Iodine added as the surfactant will be removed with sintering.

Characterizations

Sample characterizations were performed by X-ray diffraction spectroscopy with a 2θ range of 10° - 90° in Bruker DS Advance using a Cu-kα radiation of 1.5406Å with a scan rate of 5°/minute. FTIR spectroscopy with a spectral range 4000cm^{-1} - 400cm^{-1} in Thermo Nicolet iS50 was done for identification of phases. Scanning electron microscopy and with Carl Zeiss and field emission scanning electron microscopy (FESEM) with Thermo Fisher (FEI QUANTA 250 FEG) was done to observe the morphology of the particles. Raman spectroscopy was carried out by iRaman Plus (BWS465-532H) with a wavelength of 532nm. UV visible spectroscopy was carried by JASCO V-670 within wavelength range of 200 - 800 nm.

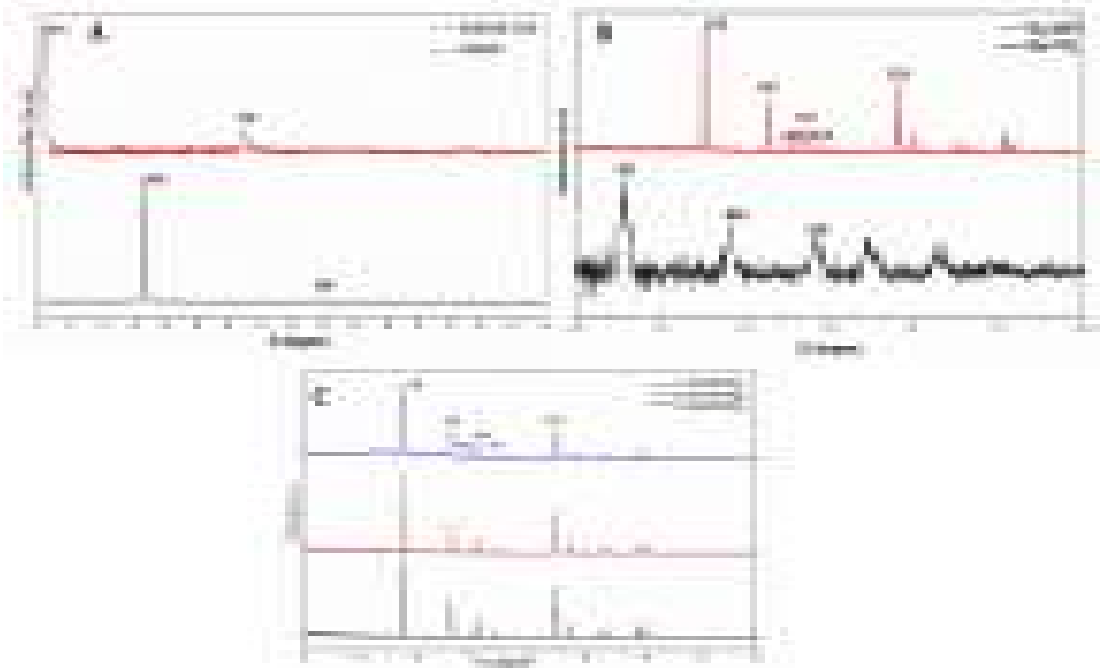

Figure 1: XRD Spectra of (a) Graphene Oxide and Graphite, (b) Raw and calcined TiO_2 (c) GO doped TiO_2 at 1wt%, 2wt% and 3wt%

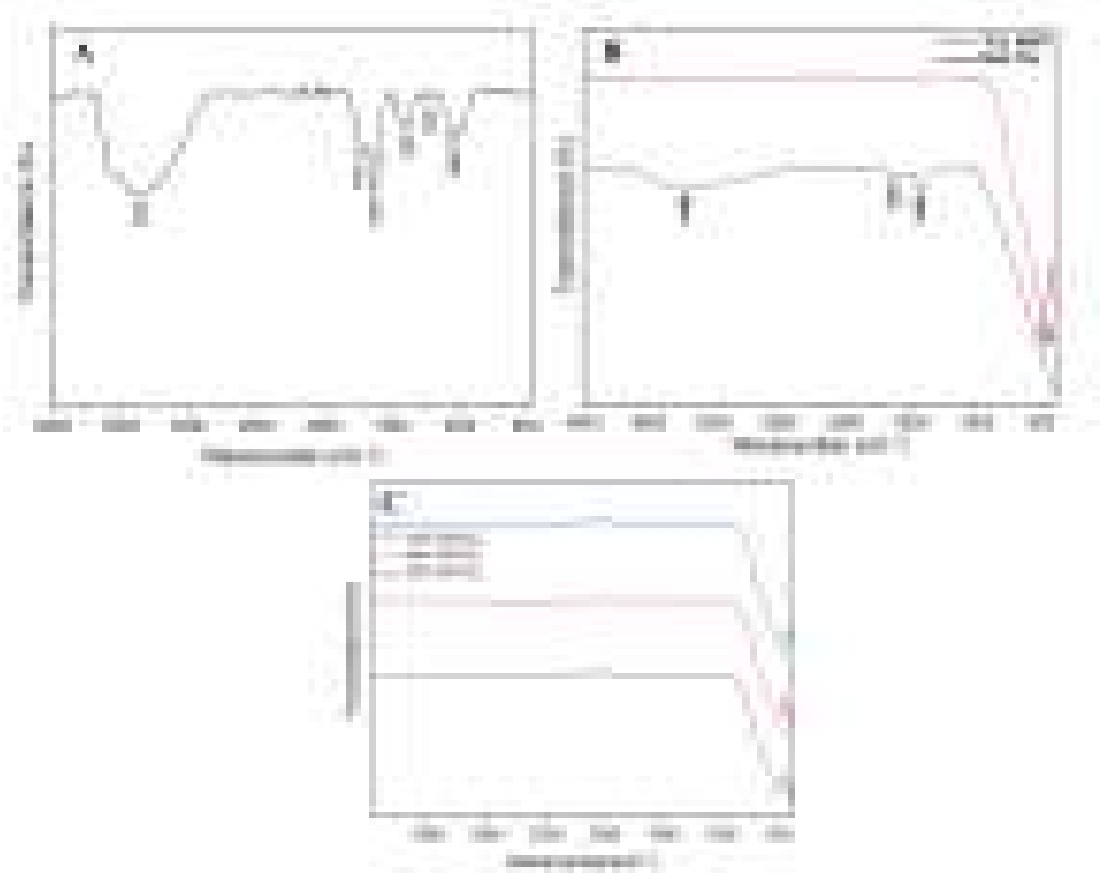

Figure 2: FITR spectra of (a) Graphene Oxide, (b) Raw and calcined TiO_2 (c) GO doped TiO_2 at 1wt%, 2wt% and 3wt%

Table 1: Heamolytic ratio of GO-TiO_2 at varying weight percentage

	TiO_2	GO-TiO_2 (1wt%)	GO-TiO_2 (2wt%)	GO-TiO_2 (3wt%)
0.5 mg/ml	1.83 ± 0.18	1.22 ± 0.06	3.56 ± 0.15	4.06 ± 0.11
1 mg/ml	3.39 ± 0.42	2.15 ± 0.20	3.97 ± 0.30	5.77 ± 0.11
2 mg/ml	4.56 ±0.43	4.61 ± 0.13	4.95 ± 0.07	7.38 ± 0.26

Photoluminescence was checked in a fluorescence spectrophotometer (HITACHI F-730). Haemolytic ratio is calculated by finding the optical density.

Results and Discussion

X-ray diffraction analysis

X-ray diffraction characterization is carried out for graphene oxide, graphite, raw and sintered TiO_2, GO-TiO_2 at different weight percentage of 1wt%, 2wt% and 3wt%. According to literature [6], GO is confirmed with a peak at $2\theta = 10°$ and reduced GO (rGO) with a peak at $2\theta = 25.4°$. From the XRD results as given in figure 1(a), we obtain a major peak at 10.72° and a minor peak at 42.51° which confirms the formation of graphene oxide at (001) and (100) planes which corroborates with existing literature [7]. Graphite gives a major peak at 26.6° and minor peak at 54.6° at (002) and (004) planes. Figure 1(b) displays the XRD pattern for raw and calcined TiO_2 at 900°C with characteristic peaks of raw TiO_2 at 2θ=24.86°, 37.4°, 47.47° and 53.95° confirming the anatase phase formation in accordance with the JCPDS card number 89-4921. As synthesized titanium dioxide yielded anatase TiO_2 which on further calcination yielded thermodynamically stable rutile TiO_2. The temperature at which phase transformation from anatase to rutile are greatly influenced by the process parameters and conditions. In our current study and previous studies, we observed the complete phase transformation of as synthesized anatase TiO_2 to pure rutile phase at 900°C [23]. The sintered TiO_2 shows rutile phase which greatly corroborates with the JCPDS card number 89-4920 with major peaks obtained at 2θ = 27.51°, 36.132°, 41.29°, 41.39°, 54.38°. This confirms the formation of TiO_2 from sol-gel synthesis. In figure 1(c), (XRD pattern) it is observed that doping of graphene oxide (varying weight percentage 1wt%, 2wt%, 3wt%) has no effect on the phase of TiO_2, it is similar to the calcined TiO_2. The calcination temperature of 900°C, which is aimed to obtain rutile phase might lead to partial transformation of GO to reduced GO [24], which is also equally beneficial as a dopant of TiO_2 dopant due to its

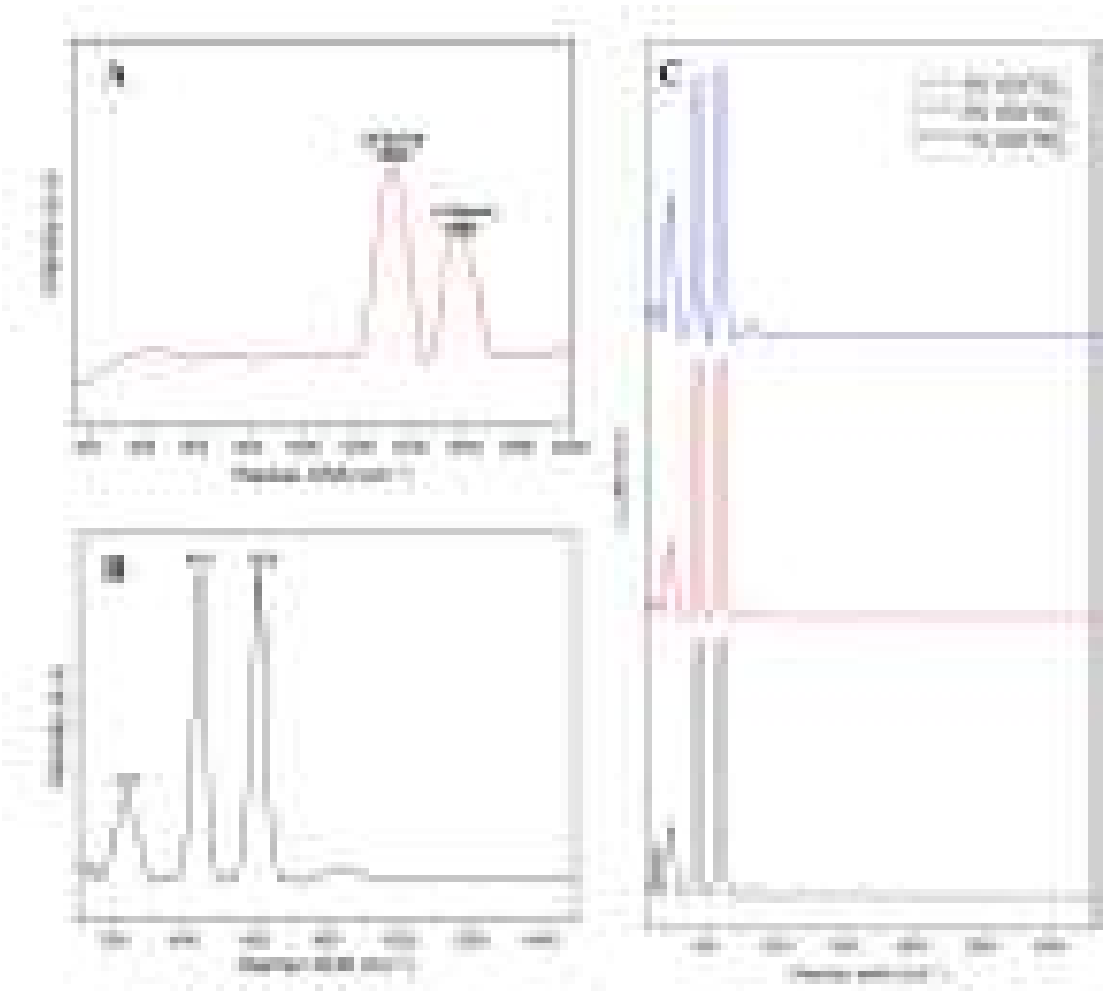

Figure 3: Raman Spectra of (a) Graphene Oxide, (b) Calcined TiO_2 (c) GO doped TiO_2 at 1wt%, 2wt% and 3wt%

improved anti-bacterial efficiency, reduced cytotoxicity, and enhanced corrosion resistance. The crystallite size (D) was calculated using Debye- Scherrer's equation, where k is Scherrer's constant, λ is the wavelength in nanometres and β is the full width half maximum (FWHM).

$$D = k\lambda / \beta\cos\theta$$

The average crystallite size after calculation was found to be 63.42nm for TiO_2 particles which suggests that the material's crystallite size lies within the nanoparticle regime. A decrease in crystallinity was observed with increased graphene oxide dopant concentration without hindering the phase transformation.

Fourier transform infrared spectroscopy

The fourier transform infrared spectroscopic analysis was carried out for the synthesized graphene oxide and titanium dioxide. The obtained data for GO as shown in figure 2(a) gave peaks at 3380 cm^{-1} for O-H stretching vibration of C-OH bonds due to the moisture content present in the material indicating the hydrophilicity of GO. 1714 cm^{-1} indicates C=O stretching in carbonyl groups, 1625 cm^{-1} for vinyl group C=C-H weak stretching, 1404 cm^{-1} indicating O-H deformation, 1229 cm^{-1} for the C-O stretching of epoxy groups, and 1048cm^{-1} for C-O stretching [25]. In figure 2(b), for raw TiO_2 the broad peak at 3200 cm^{-1} indicates the O-H peaks observed due to presence of moisture and the small peak at 1427.06 cm^{-1} indicates the Ti-OH metal hydroxide stretching mode. The calcined TiO_2 gave no peaks at 3200 cm^{-1} and the peak at 492.72 cm^{-1} indicates the Ti-O metal oxygen bending mode. Figure 2(c) shows the FTIR spectra of GO doped TiO_2 at different weight percentages, but not showing the functional groups of GO due to the very minimum dopant percentages in the parent material, even though showing a slight shift in wavenumber with increased doping indicating the changes in TiO_2 lattice due to change in Ti-O-Ti vibration.

Raman spectroscopy

Raman spectrum of TiO_2 as given in figure 3(a) shows two Raman active modes having peaks at 447 cm^{-1} and 609 cm^{-1} corresponding to E_g and A_{1g}. These peaks confirm the presence of rutile TiO_2 from previous literatures [26]. The peaks E_g and A_{1g} corresponds to symmetric stretching and anti-symmetric bending of Ti-O-Ti. The peak at 237 cm^{-1} arises as a result of multiple phonon scattering. In figure 3(b), Raman spectra of GO as given shows peaks at 1340 cm^{-1} which indicates the D band (distortion band) which denotes the distortion (sp^3 defects) caused by the oxidation process and peak at 1584cm^{-1} indicates G band (graphene band) corresponding to the sp^2 hybridised carbons [27]. From figure 3(c), peak broadening can be observed with increased doping of graphene oxide indicating increased structural disorder which means disruption in regular crystalline structure.

Scanning electron microscopy

SEM images and EDAX of polished bare titanium alloy and graphene oxide flakes are shown in figure 4. The surface morphology of the metal alloy is as important as the coating parameters. With improved surface morphology, the more the coating will get adhered to the implant. Hence, the polishing using SiC grid sheets and mirror finishing will give a smooth topography where the coating can form a uniform layer of coating. The EDAX shows the presence of titanium, aluminium and vanadium in the metal.

UV- visible spectroscopy

The UV- Visible spectrum analysis was carried out for graphene oxide and graphene oxide doped titanium dioxide. The absorbance

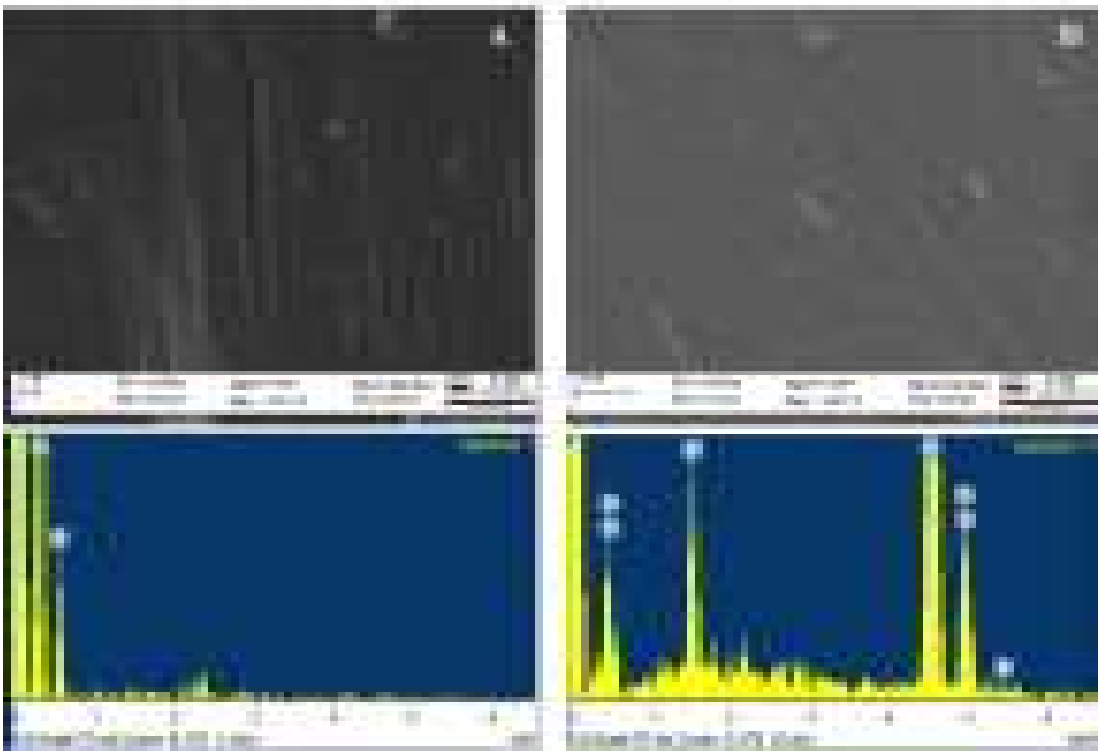

Figure 4: SEM images and EDAX of (a) Graphite flakes (b) Ti-6Al-4V bare metal

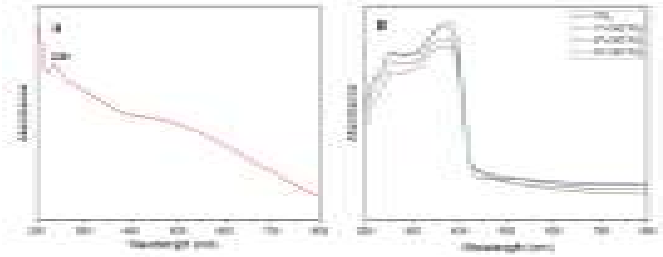

Figure 5: UV-Vis Spectra of (a) Graphene Oxide, (b) GO doped TiO_2 at 1wt%, 2wt% and 3wt%

peak was found to be at 230nm for GO (figure 5a) and a peak at 253 nm along with a broad peak at 379 nm (figure 5b) shows presence of GO doped TiO_2 TiO_2 nanoparticles respectively. The GO doped TiO_2 at 2wt% have the least absorbance value compared to the other dopant concentrations which also indirectly means band gap widening. According to literature, it is also observed that the anti-bacterial efficiency is enhanced with band gap widening [28]. Hence, from the studies we presume the graphene doped TiO_2 at 2wt% will exhibit greater anti-bacterial efficiency and hence proceeded for the electrophoretic deposition coating.

Photoluminescence

The photoluminescence property of GO and GO doped TiO_2 was analysed at 370nm. TiO_2 is proven to exhibit fair photoluminescence property [29]. With graphene oxide doping, there is quenching of photoluminescence properties in accordance to the increase in dopant concentration. As the photoluminescence is directly influential of the photocatalyst property and the reactive oxygen species generation, by lesser recombination of electrons and holes. In figure 6, it is observed that 1wt% of GO-TiO_2 doping has higher PL intensity than 2wt% and 3wt% of GO-TiO_2.

Haemolytic ratio

Haemolysis assay is proceeded in accordance with the ASTM-E2524 standard. The fresh human blood sample collected from a volunteer (Ref.No. VIT/IECH/XIII/2023/17) is centrifuged to separate the plasma to obtain the RBC pellets which is further diluted in PBS buffer is the stock solution. The samples are immersed inside the PBS buffer taken in specific amount and incubated for 1hour and further centrifuge and optical density is recorded. With the given formula, the haemolytic ratio of the compounds are carried out in triplicate, further calculated and tabulated in table 1.

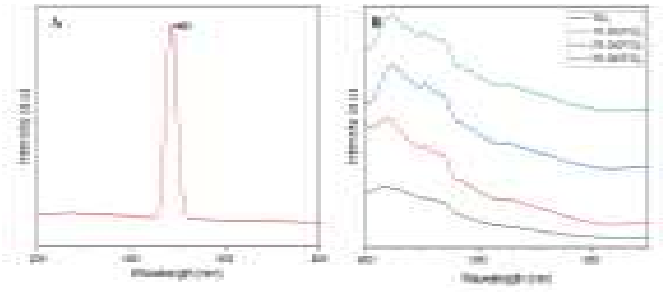

Figure 6: Photoluminescence spectra of (a) Graphene Oxide, (b) GO doped TiO_2 at 1wt%, 2wt% and 3wt%.

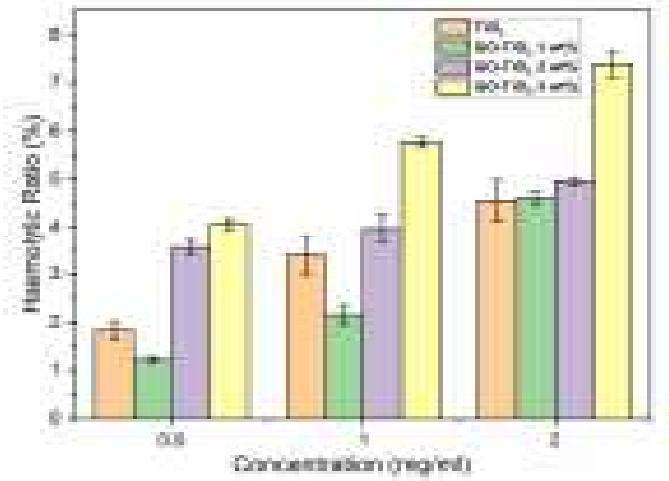

Figure 7: Illustration of haemolytic ratio (%) of TiO_2, GO doped TiO_2 at 1wt%, 2wt%, and 3wt%

Haemolytic ratio (%) = $(OD_S - OD_{NC})/(OD_{PC}-OD_{NC}) \times 100$

Where OD_S is the optical density of th sample, OD_{NC} and OD_{PC} is the optical densitis of negative control and positive control. From the calculation of haemolytic ratio, in accordance to the standard, HR < 5% is very scarcely-haemolytic, HR< 2% is non-haemolytic and HR> 5% is highly haemolytic, we select GO-TiO_2 doped at 2wt% to be optimum with scarce haemolytic effect but greater mechanical properties of graphene oxide. 3wt% is observed to show higher HR which is not recommended for bioimplant coatings. Although 1wt% GO doped TiO_2 shows least hemolysis (figure 7), the mechanical properties are also expected to be lower. In this context, we prefer 2wt% doped TiO_2 to be the optimized concentration for further studies.

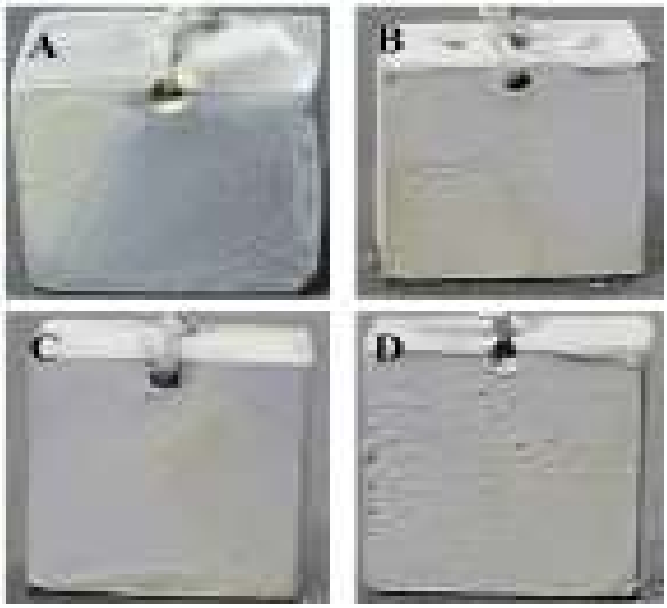

Figure 8: EPD coatings of 2wt% GO doped TiO_2 (a) 50 V, (b) 60V, (c) 70V, and (d) 80V at 180 seconds

Electrophoretic deposition coating

The optimum doping weight percentage among three, as conducted by haemolytic ratio analysis was found to be 2wt%. It was coated on the polished titanium alloys (Ti-6Al-4V), at different voltages 50V, 60V, 70V, 80V with constant timeline. 80V was found to be optimized among the four as the coating was uniform. The images of the coatings from figure 8 indicates that the surface topography is uniform and with lesser aggregation in coating with parameter 80V and 180 seconds.

Conclusions

The GO was prepared by modified hummer's method and incorporated with TiO_2 by sol-gel method with different weight percentages of 1wt%, 2wt% and 3wt%. The obtained results from XRD, FTIR, Raman and UV-Vis spectroscopy, confirmed the doping of graphene oxide into titanium dioxide. The 2wt% of GO doping was found to be optimum with scarce haemolytic property and greater anti-bacterial efficiency as presumed in accordance with the UV-Vis absorbance study and photoluminescence. Accompanying with these biological properties, they are assumed to possess great mechanical properties than 1wt% doped GO-TiO_2. Thus, optimized composition was electrophoretically deposited on titanium alloy substrate (Ti-6Al-4V) at different voltages with constant time interval. The coating was found to be optimum at 80V owing to their surface uniformity. Further, surface morphology needs to be carried out with greater resolution to observe the microstructures and its influence on coatings. As the current studies are showing potential results, the coatings could be further explored for biological and mechanical properties in detail and could effectively arise as a potent bioimplant coating.

Acknowledgement

The authors are thankful to Vellore Institute of Technology, Vellore for the instrument facilities utilized for this research work. One of the authors also thank and acknowledge the VIT Seed Grant (File no: SG20220035) for the financial support in conducting the research.

References

1. S. Jafari, B. Mahyad, H. Hashemzadeh, S. Janfaza, T. Gholikhani, L. Tayebi, Biomedical Applications of TiO_2 Nanostructures: Recent Advances, Int. J. Nanomedicine., 15, 3447–3470 (2020).
2. K. K. A. Mosas, A. R. Chandrasekar, A. Dasan, A. Pakseresht, D. Galusek, Recent Advancements in Materials and Coatings for Biomedical Implants, Gels., 8(5), 323 (2022).
3. A. Dehghanghadikolaei, B. Fotovvati, Coating Techniques for Functional Enhancement of Metal Implants for Bone Replacement: A Review., Materials, 12(11), 1795 (2019).
4. E. Cerrato, E. Gaggero, P. Calza, M. C. Paganini, The role of Cerium, Europium and Erbium doped TiO_2 photocatalysts in water treatment: A mini-review., Chem. Eng. J. Adv., 10, 100268 (2022)
5. C. Chung, Y -K, Kim, D. Shin, S. -R. Ryoo, B. H. Hong, D. -H. Min, Biomedical Applications of Graphene and Graphene Oxide. Acc. Chem. Res., 46(10), 2211–2224 (2013).
6. A. T. Habte, D. W. Ayele, Synthesis and Characterization of Reduced Graphene Oxide (rGO) Started from Graphene Oxide (GO) Using the Tour Method with Different Parameters. Adv. Mater. Sci. Eng., 1–9 (2019).
7. Ain, Q. T.; Haq, S. H.; Alshammari, A.; Al-Mutlaq, M. A.; Anjum, M. N. Beilstein J. Nanotechnol. 2019, 10, 901–911.
8. J. Prakash, K. S. K. Venkataprasanna, D. Prema, S. M. Sahabudeen, S. Debashree Banita, G. D. Venkatasubbu, Investigation on Photo-Induced Mechanistic Activity of GO/TiO_2 Hybrid Nanocomposite Against Wound Pathogens. Toxicol. Mech. Methods., 30(7), 508–525 (2020).
9. K. Lingaraju, R. B. Basavaraj, K. Jayanna, S. Bhavana, S. Devaraja, H. M. Kumar Swamy, G. Nagaraju, H. Nagabhushana, H. Raja Naika, Biocompatible Fabrication of TiO_2 Nanoparticles: Antimicrobial, Anticoagulant, Antiplatelet, Direct Hemolytic and Cytotoxicity Properties. Inorg. Chem. Commun., 127, 108505 (2021).
10. S. Y. Bhong, N. More, M. Choppadandi, G. Kapusetti, Review on Carbon Nanomaterials as Typical Candidates for Orthopaedic Coatings. SN. Appli. Sci., 1(1), 76 (2019).
11. M. Hasan Sadhir, M. Saranya, M. Aravind, A. Srinivasan, A. Siddharthan, N. Rajendran, Comparison of in situ and ex situ reduced graphene oxide reinforced electroless nickel phosphorus nanocomposite coating. Appl. Surf. Sci. 320 (30), 171-176 (2014).
12. P. Amrollahi, J. S. Krasinski, R. Vaidyanathan, L. Tayebi, D. Vashaee, "Electrophoretic Deposition (EPD): Fundamentals and Applications from Nano- to Micro-Scale Structures" in Handbook of Nanoelectrochemistry, Springer, Cham (1–27) (2015).
13. S. A. X. Stango, U. Vijayalakshmi, Electrolytic Deposition of Composite Coatings on 316L SS and its In Vitro Corrosion Resistive Behavior in Simulated Body Fluid Solution. Chem. Pap., 75(9), 4779–4791 (2021).
14. V. Balasubramani, R. Vignesh, B. Liu, T.M. Sridhar, Electrochemical impedance spectroscopic investigation on detection of H2S gas using 2D TiO2/rGO nano-composites. Appl. Surf. Sci. Adv. 16, 100415 (2023).
15. S. N. Alam, N. Sharma, L. Kumar, Synthesis of Graphene Oxide (GO) by Modified Hummers Method and Its Thermal Reduction to Obtain Reduced Graphene Oxide (rGO). Graphene., 6(1), 1–18 (2017).
16. A. Saini, A. Kumar, V. K. Anand, S. C. Sood, Synthesis of Graphene Oxide using Modified Hummer's Method and its Reduction Using Hydrazine Hydrate. Int. J. Engg. Trends. Tech., 40(2), 67–71 (2016).
17. E. H. Sujiono, Z. Zurnansyah, D. Zabrian, M. Y. Dahlan, B. D. Amin, Samnur, J. Agus, Graphene Oxide Based Coconut Shell Waste: Synthesis by Modified Hummers Method and Characterization. Heliyon, 6(8), e04568 (2020).
18. N. I. Zaaba, K. L. Foo, U. Hashim, S. J. Tan, W. -W. Liu, C. H. Voon, Synthesis of Graphene Oxide using Modified Hummers Method: Solvent Influence. Procedia. Eng., 184, 469–477 (2017).
19. U. Vijayalakshmi, M. Chellappa, U. Anjaneyulu, G. Manivasagam, Preparation and Evaluation of the Cytotoxic Nature of TiO_2 Nanoparticles by Direct Contact Method. Int. J. Nanomed. 31 (2015).
20. O. Jongprateep, R. Puranasamriddhi, J. Palomas, Nanoparticulate Titanium Dioxide Synthesized by Sol–Gel and Solution Combustion Techniques. Ceram. Int., 41, S169–S173 (2015).
21. M. Chellappa, U. Vijayalakshmi, Electrophoretic Deposition of Silica and Its Composite Coatings on Ti-6Al-4V, and its In Vitro Corrosion Behaviour for Biomedical Applications. Mater. Sci. Eng. C., 71, 879–890 (2017).
22. A. Laska, Parameters of the Electrophoretic Deposition Process and its Influence on the Morphology of Hydroxyapatite Coatings. Review. In¿ynieria Materia³owa, 1(1), 20–25 (2020).
23. Meghavathi, P. and Vijayalakshmi, U., HAp/TiO2 Composite Coatings and its Effective Use in Biomedical Applications. Trends in Biomaterials and Artificial Organs, 38(1), 5-13 (2024).
24. Liu, J., Hu, N., Liu, X. et al. Microstructure and Mechanical Properties of Graphene Oxide-Reinforced Titanium Matrix Composites Synthesized by Hot-Pressed Sintering. Nanoscale Res Lett 14, 114 (2019).
25. Bera, M., Gupta, P. and Maji, P.K., Facile one-pot synthesis of graphene oxide by sonication assisted mechanochemical approach and its surface chemistry. Journal of Nanoscience and Nanotechnology, 18(2), 902-912 (2018)..
26. L. Kernazhitsky, V. Shymanovska, T. Gavrilko, V. Naumov, L. Fedorenko, V. Kshnyakin, J. Baran, Laser-excited excitonic luminescence of nanocrystalline TiO_2 powder. Ukr. J. Phys., 59(3) 248-255 (2014).
27. J. -B. Wu, M. L. Lin, X. Cong, H. N. Liu, P. H. Tan, Raman Spectroscopy of Graphene-Based Materials and its Applications in Related Devices. Chem. Soc. Rev., 47(5), 1822–1873 (2018).
28. A. Mansoor, M. Mehmood, S. M. Hassan, M. I. Ali, M. Badshah, A. Jamal, Anti-Bacterial Effect of Titanium-Oxide Nanoparticles and their Application as Alternative to Antibiotics. Pak. Vet. J., 43(2) (2023).
29. Ruifen Wang, Kaixuan Shi, Dong Huang, Jing Zhang , Shengli An Synthesis and degradation kinetics of TiO_2/GO composites with highly efficient activity for adsorption and photocatalytic degradation of MB. Sci Rep 9, 18744 (2019).